Active Site Mutants of *Escherichia coli* Dethiobiotin Synthetase: Effects of Mutations on Enzyme Catalytic and Structural Properties

Guang Yang,[‡] Tatyana Sandalova,[§,||] Karin Lohman,[‡] Ylva Lindqvist,[§] and Alan R. Rendina*[,‡]

Dupont Agricultural Products, Stine-Haskell Research Center, P.O. Box 30, Newark, Delaware 19714-0030, Institute of Biophysics, SB RAS, 660036, Krasnoyarsk, Russian Federation, and Department of Medicinal Biochemistry and Biophysics, Karolinska Institute, S-171 77, Stockholm, Sweden

Received December 27, 1996; Revised Manuscript Received February 25, 1997[⊗]

ABSTRACT: Five active site residues, Thr11, Glu12, Lys15, Lys37, and Ser41, implicated by the protein crystal structure studies of *Escherichia coli* DTBS, were mutated to determine their function in catalysis and substrate binding. Nine mutant enzymes, T11V, E12A, E12D, K15Q, K37L, K37Q, K37R, S41A, and S41C, were overproduced in an *E. coli* strain lacking a functional endogenous DTBS gene and purified to homogeneity. Replacement of Thr11 with valine resulted in a 24 000-fold increase in the K_m(ATP) with little or no change in the K_d(ATP), K_M(DAPA) and DTBS k_{cat}, suggesting an essential role for this residue in the steady-state affinity for ATP. The two Glu12 mutants showed essentially wild-type DTBS activity (slightly elevated k_{cat}'s). Unlike wild-type DTBS, E12A had the same apparent K_M(DAPA) at subsaturating and saturating ATP concentrations, indicating a possible role for Glu12 in the binding synergy between DAPA and ATP. The mutations in Lys15 and Lys37 resulted in loss of catalytic activity (0.01% and <0.9% of wild-type DTBS k_{cat} for K15Q and the Lys37 mutant enzymes, respectively) and higher K_M's for both DAPA (40-fold and >100-fold higher than wild-type for the K15Q and Lys37 mutant enzymes, respectively) and ATP (1800-fold and >10-fold higher than wild-type for K15Q and the K37 mutant enzymes, respectively). These results strongly suggest that Lys15 and Lys37 are crucial to both catalysis and substrate binding. S41A and S41C had essentially the same k_{cat} as wild-type and had moderate increases in the DAPA and ATP K_M and K_d (ATP) values. Replacement of Ser41 with cysteine resulted in larger effects than replacement with alanine. These data suggest that the H-bond between N7 of DAPA and the Ser41 side chain is not very important for catalysis. The catalytic behavior of these mutant enzymes was also studied by pulse−chase experiments which produced results consistent with the steady-state kinetic analyses. X-ray crystallographic studies of four mutant enzymes, S41A, S41C, K37Q, and K37L, showed that the crystals were essentially isomorphous to that of the wild-type DTBS. The models of these mutant enzymes were well refined (1.9 −2.6 Å) and showed good similarity to the wild-type enzyme (rmsd of Cα atoms: 0.16−0.24 Å). The crystal structure of S41C complexed with DAPA, Mn^{2+}/Mg^{2+}, and AMPPCP revealed a localized conformational change (rotations of side chains of Cys41 and Thr11) which can account for the changes in the kinetic parameters observed for S41C. The crystal structures of the Lys37 mutant enzymes showed that the positive charge of the side chain of Lys37 is indispensable. Mutations of Lys37 to either glutamine or leucine resulted in a shift of the metal ion (up to 0.5 Å) together with side chains of other active site residues which could disrupt the subtle balance between the positive and negative charges in the active site. The conformational change of the phosphate binding loop (Gly8-X-X-X-X-Gly14-Lys15-Thr16) upon nucleotide binding observed previously [Huang, W., Jia, J., Gibson, K. J., Taylor, W. S., Rendina, A. R., Schneider, G., & Lindqvist, Y. (1995) *Biochemistry 34*, 10985] appears to be important to attain the proper active site scaffold.

Dethiobiotin synthetase (DTBS,[1] EC 6.3.3.3) catalyzes the penultimate step in the biosynthesis of the vitamin biotin in microorganisms (Eisenberg, 1973) and plants (Baldet et al., 1993). The enzyme catalyzes formation of the ureido ring of dethiobiotin (DTB) from (7*R*,8*S*)-7,8-diaminononanoic acid (DAPA) and carbon dioxide in the presence of ATP and divalent metal ions (e.g., Mg^{2+}) (Krell & Eisenberg, 1970). The reaction mechanism of *Escherichia coli* DTBS proceeds *via* the N7-carbamate of DAPA (Scheme 1) (Huang et al., 1995; Gibson et al., 1995; Alexeev et al., 1995). The proposed mechanism involves three consecutive bond-making/bond-breaking steps, which are the formation of the N7-carbamate, the formation of the mixed carbamic−phosphoric anhydride, and the ring closure of the mixed anhydride with concomitant release of inorganic phosphate (Scheme 1). The steady-state kinetic mechanism is random sequential addition of substrates (A. Rendina and K. Gibson,

* Corresponding author: telephone, 302-451-4817; FAX, 302-366-5738.
‡ Dupont Agricultural Products.
§ Karolinska Institute.
|| Institute of Biophysics.
⊗ Abstract published in *Advance ACS Abstracts,* April 1, 1997.
[1] Abbreviations: DAPA, 7,8-diaminopelargonic acid; DTB, dethiobiotin; DTBS, dethiobiotin synthetase; PEP, phosphoenolpyruvate; Na^+-Hepes, 4-(2-hydroxyethyl)-1-piperazineethanesulfonic acid sodium salt; DTT, dithiothreitol; Tris, tris(hydroxymethyl)aminomethane; Bicine, *N*,*N*-bis(2-hydroxyethyl)glycine; EDTA, ethylenediaminetetraacetic acid; IPTG, isopropyl thio-β-D-galactoside; CO_2 (unless otherwise indicated), equilibrium mixture of CO_2 and HCO_3^-; N7-DAPA-carbamate, compound formed upon addition of CO_2 to the 7-amine of DAPA; AMPPCP, adenylyl (β,γ-methylene)diphosphate; LMP, low melting point; rmsd, root mean square deviation.

S0006-2960(96)03167-4 CCC: $14.00

Scheme 1: Proposed Enzymatic Reaction Mechanism for Dethiobiotin Synthetase (DTBS) [Modified from Huang et al. (1995)][a]

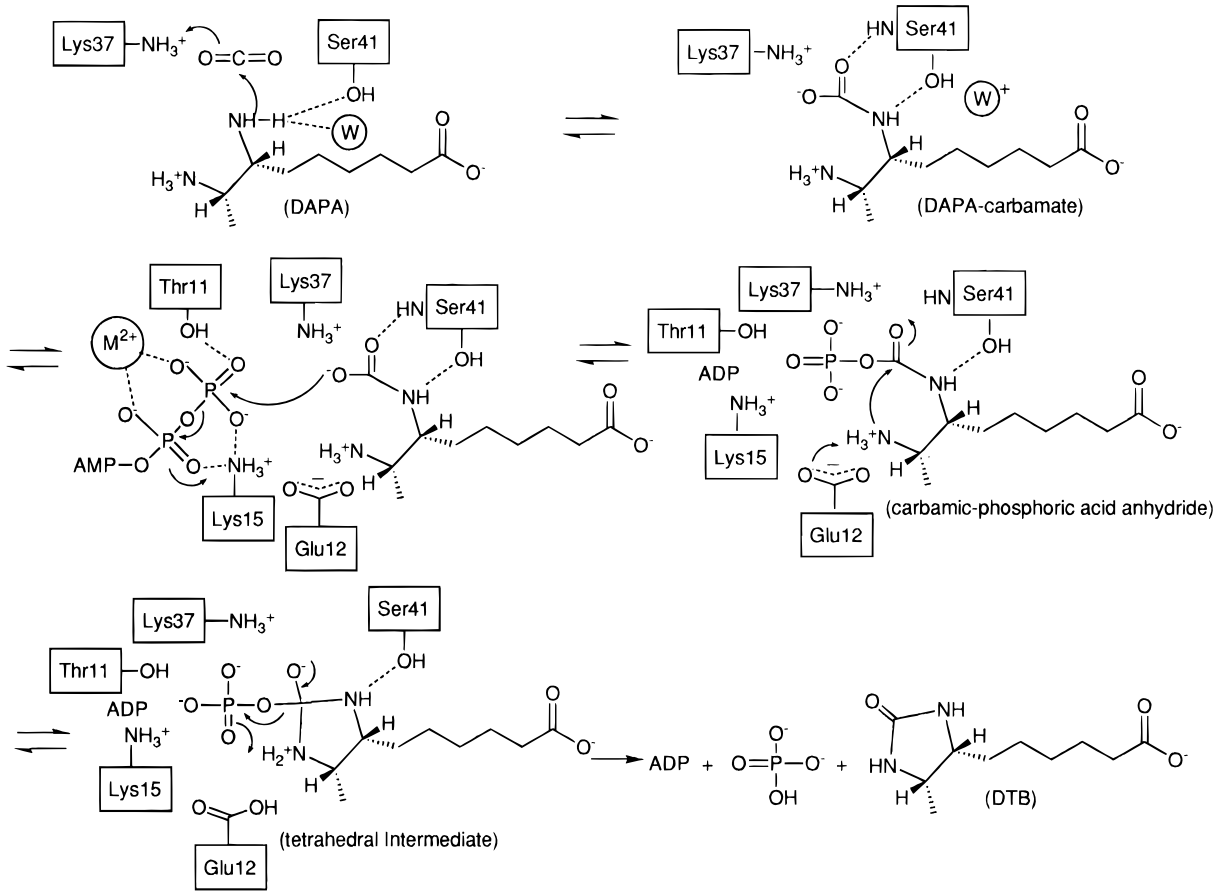

[a] M^{2+} represents the divalent metal ion at the ATP binding site. W and W^{+} represent an active site bound water molecule and its protonated form, respectively.

unpublished observations), and recent transient kinetic studies provide evidence for the carbamic−phosphoric acid anhydride intermediate (K. Gibson, personal communication). Crystallographic studies of *E. coli* DTBS complexes with substrates and a reaction intermediate analog [3-(1-aminoethyl)nonanedioic acid] have implicated five active site amino acid residues (Thr11, Glu12, Lys15, Lys37, and Ser41) functioning in each of the three reaction steps and playing essential roles in catalysis and binding of substrates (Huang et al., 1995). The positive side chains of the two lysine residues and the hydroxyl side chains of Thr11 and Ser41 were proposed to be important in the binding of the substrates and stabilization of the reaction intermediates along the reaction pathway, while the Glu12 residue was postulated to serve as a general catalytic acid in the phosphate transfer step and/or a general base in the ring closure steps (the later is illustrated in Scheme 1). In addition, Thr11, Lys15, and Lys37 are conserved residues in all sequences of DTBS reported to date, and Ser41 is conservatively replaced with a threonine in some sequences. In contrast, we have recently found that Glu12 is not conserved in all DTBS sequences.[2]

The goals of the present investigation are to evaluate the proposed functions of these active site enzymic residues and to gain more insight into this unique enzyme system. Site-directed mutagenesis is used to individually replace the five postulated active site residues with different amino acids. The resulting mutants of DTBS are characterized in this paper by steady-state kinetic analysis, pulse−chase experiments, substrate binding assays, and X-ray crystallography.

MATERIALS AND METHODS

General. DNA sequencing was carried out using the ultra pure SEQUALGEL-6 from National Diagnostic and the USB DNA Sequenase kit (version 2.0). Electrospray mass spectrometry data were collected on a Fisons VG Quattro II instrument. Enzyme assays were carried out on a Uvikon 940 spectrophotometer. Radioactivity assays were performed on a Beckman LS 3801 scintillation counter. Fluorescence scans were carried out on an SLM-AMINCO spectrofluorimeter (model SLM8000). DAPA was prepared from dethiobiotin as described in Gibson et al. (1995). All other reagents and chemicals were of the highest commercially available quality.

Construction of the Recombinant DTBS Expression System. The Novagen *p*ET system was used in the overexpression of the recombinant DTBS proteins. A new clone (*pbio*D), using *p*ET 21 as the expression vector and containing only the *bio*D (DTBS) gene, was constructed to give high yields of soluble, recombinant *E. coli* DTBS protein. Since the expression of the genomic DTBS from the host BL21(DE3) strain (Novagen) could contaminate low activity mutants of DTBS, a mutant BL21(DE3) strain, BL21(bioD::NPTII,

[2] Glu12 is conservatively replaced with aspartate in homologous enzymes from many species but is not conserved in DTBS from blue-green algae (*Synechocystis* sp.), *Haemophyllis influenza*, or *Bacillus sphaericus* (J. Chen, S. Vollmer, and A. Rendina, unpublished observations). The sequences for *H. influenza* and *Synechocystis* sp. were not available until after the mutagenesis work began.

DE3), which contains a defective DTBS gene (bioD), was prepared. For details of these preparations, see Supporting Information.

Site-Directed Mutagenesis. Site-directed mutants were prepared from the DTBS gene in plasmid *pbio*D (see above) using the methodology described in Erlich (1992). PCR reactions were carried out in a Perkin-Elmer Thermalcycler using template DNA (prepared using a Wizard Minipreps DNA purification system supplied by Promega), synthetic primers (supplied by Oligos, Inc.), and the PCR reagents supplied in the Perkin-Elmer Cetus GeneAMP kit. Each 100 μL reaction contained 50 mM KCl, 10 mM Tris-HCl (pH 8.3), 200 μM each of dATP, dCTP, dGTP, and dTTP, 20 pM each of primer, 2.5 units of Taq DNA polymerase, 4 mM $MgCl_2$, and 0.5 μg of template DNA. The actual base substitutions, location of primers, and restriction enzymes used are shown in Table 1 of the Supporting Information. Reaction mixtures were overlaid with 50 μL of sterile silicone oil. Following each reaction, the sample was electrophoresed on a 0.8−1.2% LMP agarose (Gibco BRL) gel, and the DNA was extracted using the Geneclean II kit (Bio 101). The DNA of the mutated region and the *pbio*D clone were digested with *Sac*I and *Not*I restriction enzymes (Promega) and purified by LMP agarose electrophoresis. Following T4 DNA ligase (New England Biolabs) catalyzed ligation of the mutant fragment to the cut plasmid *pbio*D, the clone was transformed into competent BL21(bioD::NPTII, DE3) cells (Sambrook et al., 1989). The sequence of the resulting mutated *pbio*D plasmid in the region manipulated was verified by chain termination methods (Sanger et al., 1977) using the Sequenase DNA sequencing kit from United States Biochemicals. The molecular weight of the overexpressed mutant DTBS proteins was confirmed by electrospray mass spectrometry standardized with myoglobin and wild-type DTBS protein (Table 1).

Purification of Recombinant Proteins. Wild-type and mutant proteins were purified from the newly constructed *E. coli* BL21(bioD::NPTII, DE3, *pbio*D) strain (see above) using a modified procedure of Gibson et al. (1995). After cell harvesting (typically 15 g of wet cell paste) and cell lysing by a French press, the cell-free extract was directly chromatographed on a 90 mL Q-Sepharose Fast Flow (Pharmacia) column (2.5 × 20 cm). The column was developed with a linear gradient of 0−0.5 M NaCl in a total volume of 800 mL of 50 mM Na^+Hepes buffer (pH 7.5, containing 1 mM DTT and 0.1 mM EDTA) at a flow rate of 3 mL/min. Fractions containing DTBS were determined by absorption measurement at 280 nm and SDS−PAGE gel analysis. After DTBS fractions were pooled, ammonium sulfate was added to a final concentration of 10%, and the protein solution was applied to a 20 mL phenyl-Sepharose Fast Flow (Pharmacia) column (1.5 × 20 cm). The DTBS protein was eluted using a gradient of 10−0% ammonium sulfate in a total volume of 400 mL of 50 mM Na^+Hepes buffer (pH 7.5, containing 0.1 mM EDTA) at a flow rate of 1.5 mL/min. Fractions containing high concentrations of DTBS protein ($A_{280} \geq 0.8$) were analyzed for purity by SDS−PAGE. Fractions containing pure DTBS were pooled, dialyzed against 20 mM Na^+Hepes buffer (pH 7.2), and concentrated, yielding *ca*. 100 −150 mg of DTBS from 15 g of wet cell paste.

Steady-State Kinetic Measurement of Wild-Type and Mutant DTBS. The kinetic parameters K_m and k_{cat} of ATP and DAPA with each enzyme were determined from the initial velocity data measured by limiting one substrate and saturating with the others.[3] For rapidly turning over mutant enzymes and wild-type DTBS, the activity was measured spectrophotometrically by monitoring ADP formation using the pyruvate kinase/lactate dehydrogenase coupled assay (Cleland, 1979a). The decrease in the absorbance ($\Delta\epsilon$ = 6.22 $mM^{-1}\cdot cm^{-1}$ at 340 nm) of a 0.5 mL assay solution was used to calculate the initial velocity. For slowly turning over mutant enzymes, the activity was determined by the [^{14}C]-CO_2 fixation assay described previously (Gibson et al., 1995). The time course of the formation of DTB was measured directly by monitoring the incorporation of [^{14}C]CO_2 using [^{14}C]$NaHCO_3$ (New England Nuclear, 11.1 mM, 0.5 mCi/mL) into [^{14}C]DTB. Specific radioactivity of the [^{14}C]CO_2 in a reaction assay was typically 1.43×10^2 dpm/nmol. Data were analyzed using eq 1 and the FORTRAN programs of

$$V_0 = V_m[A]/([A] + K_M) \quad (1)$$

Cleland (1979b) adapted for a PC. In eq 1, V_0 = initial velocity, V_m = maximal velocity, [A] = limiting substrate concentration, and K_M = Michaelis constant. The k_{cat} values were determined from the V_m values and total enzyme concentration used in the reaction according to the equation $k_{cat} = V_m/[E]$. DTBS concentrations were calculated using ϵ = 37.5 $mM^{-1}\cdot cm^{-1}$ at 280 nm (Gibson et al., 1995).

ATP Binding to Wild-Type and Mutant DTBS. The dissociation constants (K_d) of ATP were determined for the wild-type and mutant DTBS proteins by a modification of the ultrafiltration method described by Ormö and Sjöberg (1990). The binding experiment was carried out using an Ultrafree-MC filter unit with a regenerated cellulose membrane (molecular weight cutoff 10 000; Millipore) at 25 °C in a buffer containing 80 mM Hepes, pH 7.5, and 5 mM $MgCl_2$. [8-^{14}C]ATP (specific activity 1.2×10^5 dpm/nmol, 0.910 mM) purchased from New England Nuclear was diluted to a specific activity of 1.0×10^4 dpm/nmole (for low K_d wild-type and mutant enzymes) and 3.5×10^3 dpm/nmol (for high K_d mutant enzymes) with more than 90% pure ATP from Sigma to generate final ATP concentrations of 218.2 μM and 3.091 mM, respectively. The concentration of ATP in a binding experiment was typically 3.6−57 μM. For mutants with high K_d values (K15Q, Lys37 mutants, and S41C), the ATP concentration was increased to 51.5−824 μM. The amount of enzyme in the assay (13−150 μM or 40−900 μg of protein in a final volume of 150 μL depending on the K_d) was chosen so that the amount of bound ATP was 10%−80% of the total ATP. For a typical binding experiment, the components were mixed and then incubated for 15 min at ambient temperature. An aliquot of 30 μL was withdrawn for scintillation counting to determine the total ATP concentration, and 100 μL of the remaining 120 μL was transferred to the upper sample reservoir of the Ultrafree-MC filter unit. After centrifugation at 16000*g* for 2−3 min in an Eppendorf centrifuge (model 5415C) at ambient temperature, an aliquot of 30 μL was withdrawn from the filtrate volume (approximately 40 μL) for scintil-

[3] Saturating conditions for CO_2 in the DTBS activity assays were achieved by using 15 mM $NaHCO_3$ at pH 7.5. This was further confirmed by measuring the V_{max} of DTBS for the wild-type and mutant enzymes at 15 and 105 mM $NaHCO_3$ concentrations, which correspond to 0.6 and 3.9 mM CO_2 at pH 7.5.

lation counting and calculation of the free ATP concentration. The amount of bound ATP was calculated as the difference between total and filtrate ATP concentration. K_d's were calculated by linear regression analysis from the reciprocal of the slope of a Scatchard plot (bound ATP/free ATP versus bound ATP).

Pulse−Chase Experiments. For the pulse−chase experiments [modified from Gibson et al. (1995); see also Rose (1980)], three different concentrations of enzyme (wild-type or mutants) were preincubated (pulsed) with saturating amounts of [^{14}C]$NaHCO_3$ and DAPA for 20 min at ambient temperature and then quickly mixed with saturating levels of ATP and a large excess of unlabeled $NaHCO_3$ to initiate the DTBS reaction (chased). Incorporation of label into final product (DTB) at different time points was monitored by radioactive assay on a scintillation counter. Typically, an 1.28 mL "pulse" solution contained 125 mM Na^+Bicine (pH 7.85), 12.5 mM $MgCl_2$, 6.26 mM [^{14}C]$NaHCO_3$ (prepared by dilution of the 11.1 mM [^{14}C] $NaHCO_3$ stock from New England Nuclear, 0.5 mCi/mL, with unlabeled 1.0 M $NaHCO_3$ solution), 500 μM DAPA, 37.5 ng/μL carbonic anhydrase, and DTBS active site concentrations near 10, 20, and 30 μM for the wild-type, T11V, E12A, E12D, S41A, and S41C enzymes and near 30, 60, and 90 μM for the K37L and K37Q enzymes. The 320 μL "chase" solution contained 3 or 132.7 mM ATP and 500 mM unlabeled $NaHCO_3$. Two different concentrations of ATP (final concentrations: 0.6 and 26 mM) were used to ensure saturation in the chase phase. Aliquots (100 μL) were quenched with 20 μL of 6 M HCl at defined time points of 10, 20, 30, 40, 50, 60, 70, 80, 90, 100, 120, 140, 160, 180, and 200 s for wild-type, T11V, E12A, E12D, S41A, and S41C enzymes and of 2, 4, 6, 8, 10, 12, 14, 16, 18, 20, 30, 40, 50, 60, and 80 min for the K37L and K37Q enzymes. A total of 100 μL of the quenched mixture was then transferred into a glass vial and taken to dryness in a vacuum oven to remove unreacted [^{14}C]-CO_2. The residue was dissolved in 0.5 mL of water, 10 mL of EcoLume (ICN) was added, and the ^{14}C radioactivity was determined by scintillation counting. The radiospecific activity of the [^{14}C]CO_2 in the preincubation was used to compute the quantiity of [^{14}C]DTB formed at each time point. The data were plotted as nanomoles of DTB versus time at each enzyme level, and the intercepts were determined by linear regression analysis of the steady-state region (60−200 s for WT, E12A, E12D, S41A, and S41C; 10−50 s for T11V; and 2−20 min for K37L and K37Q). The replot of these "burst intercepts" versus enzyme concentration was linear for the wild-type and the tested mutant enzymes. The slope of these replots is the stoichiometry of N7-DAPA-carbamate that becomes committed to DTB formation upon addition of ATP [see Figure 5 of Gibson et al. (1995)].

Crystallization and Data Collection. Crystals of DTBS mutants (K37L, K37Q, S41A, and S41C) were obtained as described earlier (Huang et al., 1994). Crystals of complexes of mutants of DTBS with DAPA, Mn^{2+} or Mg^{2+}, and AMPPCP as well as complexes of the S41A and S41C mutants with DAPA and Mn^{2+} were prepared by soaking native crystals for 10−24 h in the crystallizing reservoir solution containing 5 mM DAPA and/or 5 mM AMPPCP in the presence of either 100 mM $MnCl_2$ or 100 mM $MgCl_2$ as described (Huang et al., 1995). Crystals of mutants are isomorphous to the native crystals, space group *C*2, and cell dimensions of $a = 73.2$ Å, $b = 49.2$ Å, $c = 61.8$ Å, and $\beta = 107.1°$. Diffraction data sets were collected at room temperature on a Rigaku rotating anode at 50 kV and 90 mA, and data were processed with DENZO/SCALEPACK (Otwinowski, 1993). One crystal of every mutant was used for each data set. Details of the data collection are given in Table 6. Initial phases were calculated from the coordinates of the respective complexes of the wild-type enzyme (Huang et al., 1995). Model building of the mutants was made with the program O (Jones et al., 1991), and crystallographic refinement was carried out with X-PLOR (Brunger, 1990).

RESULTS

Expression of Recombinant DTBS in BL21(bioD::NPTII, DE3) and Site-Directed Mutagenesis. Since the T7 RNA polymerase-producing host strain [BL21(DE3)] used in the expression of recombinant DTBS had its own genomic DTBS gene which could contaminate preparations of DTBS mutants, a mutant BL21 strain, BL21(bioD::NPTII, DE3), was constructed by insertional mutagenesis of the endogenous DTBS gene (see Materials and Methods). The *pbio*D, as described below, was shown to produce the same level of soluble wild-type DTBS in either the BL21(bioD::NPTII, DE3) strain or the original BL21(DE3) strain as estimated by SDS−PAGE of cell-free extracts of the two strains (data not shown). As previously demonstrated, the original recombinant DTBS plasmid, *pbio*CD, containing both *bio*C and *bio*D (DTBS gene) genes under transcriptional control of a T7 promoter, produced both the *bio*C protein (28 kDa) and DTBS (24 kDa) in mostly insoluble forms (Gibson et al., 1995). On the basis of the SDS−PAGE analysis of whole cells, cell-free extracts, and the precipitated cell debris of the *pbio*CD clone, we noticed that expression of *bio*C protein was much higher than expression of DTBS (data not shown). Moreover, while at least 10% of the expressed DTBS was soluble, almost all of the *bio*C protein formed inclusion bodies. This suggested that the expression of *bio*C interfered with the expression of the *bio*D (DTBS) gene and that the partial precipitation of the 24 kDa DTBS enzyme might be affected by the aggregation of the 28 kDa (*bio*C) protein. We thus recloned the DTBS gene (*bio*D) by excising the *bio*D gene fragment from *pbio*CD and ligating it into a Novagen transcriptional vector, pET21. A transcriptional vector was possible because the fragment of *pbio*CD excised by *Sac*I and *Not*I contained both the bioD gene and its own ribosome binding site. After transformation into the host strain and induction with IPTG, the new clone (*pbio*D) produced completely soluble DTBS proteins with a higher yield. With the new recombinant DTBS expression system, it was feasible to obtain a large quantity of pure recombinant DTBS enzyme with no contamination by DTBS activity from the host strain.

Five enzymic residues in the *E. coli* DTBS active site, Thr11, Glu12, Lys15, Lys37, and Ser41, were selected for amino acid replacement. Thirteen mutant genes of these five residues, T11A, T11V, E12A, E12D, K15L, K15Q, K15R K37L, K37Q, K37R, S41A, S41C, and S41D, were constructed by PCR and expressed using the vectors described above. The T11V, E12A, E12D, K15Q, K37L, K37Q, K37R, S41A, and S41C mutant enzymes were purified to homogeneity; the T11A mutant DTBS was not inducible with IPTG; and the K15R and S41D mutant enzymes were found to form inclusion bodies. The nine purified mutant enzymes were characterized as described below.

Table 1: Molecular Mass of the Wild-Type and Mutant *E. coli* Dethiobiotin Synthetases (DTBS) Measured by Electrospray Mass Spectrometry[a]

DTBS enzymes	molecular mass (Da) by electrospray, MS	molecular mass (Da) predicted by amino acid sequence
wild type	24006.6	24008.2
T11V	24004.6	24006.2
E12A	23947.4	23950.2
E12D	23992.8	23994.2
K15Q	24006.2	24008.2
K37L	23991.4	23990.2
K37Q	24006.3	24008.2
K37R	24034.2	24036.1
S41A	23990.3	23992.2
S41C	24022.6	24024.3

[a] About 4 μL of 24 μM DTBS protein in acetonitrile/water/formic acid (50%/50%/0.5%) solution was used in the measurement. The instrument was calibrated with a myoglobin standard. The estimated error of the molecular mass for each protein is within 0.01%.

Physical Properties of the T11V, E12A, E12D, K15Q, K37L, K37Q, K37R, S41A, and S41C Mutant DTBS's. To verify that the intended mutations were obtained, the manipulated region of the DNA was sequenced (see Materials and Methods), and the subunit molecular mass of the mutant enzymes was determined by electrospray mass spectrometry and was in good agreement with the value predicted from the amino acid sequence (Table 1). In addition, the crystallographic data in K37L, K37Q, S41A, and S41C confirmed the changes at the designated sites.

Proper folding of the mutant enzymes was established by the following criteria: (1) The expression levels of these mutant enzymes were comparable to that of the wild-type DTBS based on SDS−PAGE; (2) all the mutant enzymes were purified on Q-Sepharose and phenyl-Sepharose columns in the same manner as used for the wild-type DTBS; (3) SDS−PAGE analysis and fluorescence emission spectra showed that the mutant enzymes displayed essentially the same resistance to proteolysis during purification and storage, and the same emission maximum at 330 nm when the mutant enzyme solutions were excited at 295 nm as the wild-type DTBS; and (4) X-ray structures of K37L, K37Q, S41A, and S41C showed good similarity of these mutants to the wild-type DTBS (see below).

Steady-State Kinetic Properties of the Mutant Enzymes. The DTBS activities of the mutant enzymes were examined using either the spectrophotometric assay (for wild-type, Thr11, Glu12, and Ser41 mutant enzymes) or the [^{14}C]CO_2 fixation assay (for Lys15 and Lys37 mutant enzymes) to monitor the formation of ADP and [^{14}C]DTB, respectively, under steady-state conditions (Gibson et al., 1995). At saturating levels of CO_2, initial velocity kinetic techniques were used to measure K_M and k_{cat} values of the wild-type and mutant DTBS enzymes for both ATP and DAPA (see Table 2).

The T11V mutant DTBS had a 24 000-fold higher K_M (ATP) than wild-type with no significant change in the k_{cat} or K_M (DAPA), suggesting that the Thr11 residue in the DTBS active site is important for binding of ATP in the presence of the other substrates and for the catalytic efficiency (k_{cat}/K_M) with respect to ATP. Compared to the wild-type DTBS, the two Glu12 mutant DTBS's showed slightly elevated k_{cat}'s and essentially the same K_M values for both ATP and DAPA, indicating that the Glu12 residue was not important for either catalysis or binding of ATP and DAPA.

The turnover rate (k_{cat}) for the K15Q mutant DTBS was 0.01% that of the wild-type enzyme, and its K_M values for DAPA and ATP were 50-fold and 1800-fold higher, respectively, than those of the wild-type DTBS. These results clearly showed that Lys15 was crucial for both catalysis and binding of DAPA and ATP with a more severe effect on the binding of the later substrate. Similarly, Lys37 was shown to be important for both catalysis and binding of substrates by the three Lys37 mutant enzymes, which exhibited at least 100-fold and 10-fold increases in the K_m of DAPA and ATP, respectively, and had no greater than 0.8% of the turnover rate of the wild-type DTBS. The less dramatic increase in the K_M(ATP)'s than in the K_M (DAPA)'s for the Lys37 mutant DTBS's suggested a more important role for Lys37 in the binding of DAPA.

The turnover rates for the two Ser41 mutant DTBS's were essentially wild type like. While both Ser41 mutant enzymes showed about 6-fold increases in the K_M(ATP)'s, only the S41C mutant DTBS showed an elevated K_M(DAPA) (about 6-fold). These results indicate that Ser41 is not as important to catalysis as suggested by the crystal structure studies (Huang et al., 1995).

The apparent K_M(DAPA) for the Glu12 and Ser41 mutant DTBS's was also measured at subsaturating ATP concentrations (1 μM ATP) using the spectrophotometric assay (Table 3). The Glu12 mutant enzymes showed essentially the same apparent K_M (DAPA) as the wild-type enzyme at subsaturating ATP, indicating that Glu12 is not important for binding DAPA. However, unlike wild-type DTBS, the same apparent K_M values were observed at *both* saturating and subsaturating ATP concentrations for the E12A DTBS, suggesting that this residue may be important for the synergistic binding ($K_M \ll K_{ia}$) of DAPA and ATP which has been demonstrated previously (Gibson et al., 1995). Both Ser41 mutant DTBS's showed 4- and 6-fold (for S41A and S41C, respectively) increases in the apparent K_M(DAPA) at subsaturating ATP, implying that the Ser41 residue had a more important role in binding of DAPA in the absence of ATP.

Pulse−Chase Experiments with Mutant Enzymes. In these experiments, the amount of the binary complex of DTBS·N7-DAPA-carbamate committed to DTB formation upon addition of saturating levels of ATP was determined. As is the case with wild-type DTBS (Gibson et al., 1995), a burst of [^{14}C]DTB formation was observed for the T11V, E12A, E12D, S41A, and S41C DTBS's after a preincubation solution of the mutant enzymes, DAPA, [^{14}C]CO_2, and $MgCl_2$ was mixed with ATP and excess unlabeled CO_2. The burst amplitudes for these mutant enzymes were also proportional to the DTBS concentration. Except for the T11V and S41C mutant DTBS's, the stoichiometry of the committed binary complex (DTBS·N7-DAPA-carbamate) for the wild-type DTBS and the other tested mutant DTBS's was about the same (Table 4). The results show that these DTBS mutants, E12A, E12D, and S41A, retain the same forward commitment to catalysis as the wild-type enzyme. With S41C the amount of committed binary complex trapped was 3.7-fold less than wild-type DTBS, consistent with the elevated K_m's for DAPA and ATP.

The time course for the pulse−chase experiments with T11V was complex. Instead of a burst followed by steady-

Table 2: Kinetic Parameters (K_m, k_{cat}) for the Wild-Type and Mutant DTBS Enzymes (pH 7.5, 25 °C) Measured by Spectrophotometric Assay and [^{14}C]CO_2 Fixation Assay

enzymes	k_{cat}[c] (min^{-1})	K_m[c] (DAPA) (μM)	k_{cat}/K_m(DAPA) ($M^{-1}\cdot s^{-1}$)	K_m(ATP) (μM)	k_{cat}/K_m(ATP) ($M^{-1}\cdot s^{-1}$)
wild type[a]	3.73	0.30	2.07×10^5	0.39	1.59×10^5
T11V[a]	1.51	0.34	7.40×10^4	9.47×10^3	2.65×10^0
E12A[a]	4.61	1.13	6.82×10^4	0.33	2.33×10^5
E12D[a]	6.97	0.23	5.05×10^5	2.38	4.88×10^4
K15Q[b]	5.4×10^{-4}	11.1	8.10×10^{-1}	7.01×10^2	1.29×10^{-2}
K37L[b]	2.6×10^{-2}	30.8	1.41×10	4.30	1.01×10^2
K37Q[b]	3.2×10^{-2}	30.4	1.75×10^1	4.53	1.18×10^2
K37R[b]	2.9×10^{-3}	143	3.38×10^{-1}	7.44	6.50×10^0
S41A[a]	3.83	0.28	2.28×10^5	2.24	2.85×10^4
S41C[c]	3.29	1.68	3.27×10^4	1.45	3.78×10^4

[a] Measured by spectrophotometric assay. [b] Measured by [^{14}C]CO_2 fixation assay. [c] The estimated errors for K_m and k_{cat} are within ±15%.

Table 3: Comparison of Kinetic Parameters for the Wild-Type DTBS and Glu12 and Ser41 Mutant Enzymes at Saturating (3 mM) and Subsaturating (1 μM) ATP Concentrations at pH 7.5, 25 °C[a]

	apparent V_{max}(DAPA) (min^{-1})		apparent K_m(DAPA) (μM)	
DTBS enzymes	saturating ATP	subsaturating ATP	saturating ATP	subsaturating ATP
wild type	3.73	1.67	0.30	3.15
E12A	4.61	2.59	1.13	1.29
E12D	6.97	1.79	0.23	2.88
S41A	3.83	1.69	0.28	11.6
S41C	3.29	1.79	1.68	19.7

[a] The estimated errors for apparent K_m's and V_{max}'s are within ±15%.

Table 4: Summary of Pulse−Chase Experiments with Wild-Type and Mutant Enzymes at 26.5 mM ATP (Final)[a]

DTBS enzymes	slope of burst intercept replot (DTBS·DAPA·CO_2 complex/active site)
wild type	0.86
T11V[b]	0.27
E12A	1.06
E12D	0.82
K37L	0.01
K37Q	0.01
S41A	0.76
S41C	0.23

[a] The estimated error is ±10% for the values of the slope. [b] The burst intercepts for T11V were measured by extrapolation of the lag phase of the time course of [^{14}C]DTB formation in the isotope partition experiments to the zero time point (see text for details).

state [^{14}C]DTB formation as observed for wild-type DTBS, T11V DTBS had a rapid burst followed by a lag and then a steady-state phase. The rapid burst amplitude was measured by extrapolation of the lag phase to zero time and was proportional to enzyme concentration. By this analysis, the forward commitment to catalysis for the T11V mutant DTBS was reduced by 3.2-fold compared to wild-type DTBS.

For two Lys37 mutant DTBS's, K37L and K37Q, a steady-state formation of [^{14}C]DTB with a negligible burst phase was observed for the time range 2−80 min at either 0.6 or 26.5 mM final ATP levels, suggesting that no *committed* binary complex (DTBS·DAPA-carbamate) was formed in the preincubation mixture of K37L and K37Q with DAPA-carbamate. Note that the level of ATP in the chase may not have been high enough to trap the binary complex because of the very poor catalytic efficency of these mutants with respect to ATP (Table 2) (Rose, 1980). No pulse−chase experiments were carried out for K15Q and K37R because of their extremely slow turnover rates (Table 2).

ATP Binding to Free DTBS Proteins. The binding of ATP to free enzyme for both wild-type and mutant enzymes was measured by an ultrafiltration method. The K_d values are summarized in Table 5. With the exception of T11V and E12A, all the mutant enzymes showed an elevated K_d for ATP with S41C, K15Q, and the three Lys37 mutant DTBS's having larger increases. These results were consistent with the steady-state kinetic measurements. The T11V mutant DTBS had essentially the same K_d as the wild-type DTBS, whereas the E12A mutant DTBS displayed a 6-fold *tighter* binding of ATP.

Structural Properties of K37L, K37Q, S41A, and S41C Mutants. The crystal structures of four different mutants of DTBS were determined: S41A, S41C, K37Q, and K37L in complexes with DAPA, Mn^{2+}/Mg^{2+}, and AMPPCP (an analogue of ATP). In addition, the crystal structures of the binary complexes of S41A and S41C with DAPA and Mn^{2+} were also solved. Table 6 shows that these mutant enzymes are well-refined protein models. All of them are very similar to the wild-type enzyme: root mean square deviations (rmsd) between all Cα atoms of the mutant and native enzyme complexes are between 0.16 and 0.24 Å. This indicates that the mutations do not affect the fold of DTBS and do not result in any large conformational changes. Mutated residues have very good electron density and correspond to the predicted side chains.

The electron density of bound AMPPCP is clearly seen in all mutant complexes just at the place where it is bound to wild-type enzyme. All studied mutants have poor electron density for DAPA compared to the wild-type protein complexes, even though crystals were soaked at a 200−1000 times excess of DAPA during 10−24 h. The carboxyl termini of DAPA are well defined in electron density while the electron density for the diamino part is poor for S41A and worse in S41C, and no electron density $>1.0\sigma$ was found for the diamino part of DAPA in the Lys37 mutants. No trace of carbamylated DAPA was observed in any of the mutants, not even in S41A which had the best occupancy for DAPA. Addition of $NaHCO_3$ to the solution during soaking also did not result in occupancy of the carbamate site in either the binary or ternary complexes. In wild-type DTBS, carbamylated DAPA was bound in the active site after this treatment in the presence of Ca·AMPPCP, but not Mn·AMPPCP, and was present in all binary complexes with DAPA (Huang et al., 1995). It appears that DAPA binding occurs in all four mutants but the substrate is not rigidly held in the active site of DTBS after mutation of either Ser41 or Lys37, and therefore, cannot be well defined in electron

Table 5: Dissociation Constants (K_d) for Wild-Type (WT) and Mutant DTBS Complexes of Mg·ATP Determined at pH 7.5 and 25 °C[a]

	K_d (μM)									
ligand	WT	T11V	E12A	E12D	K15Q	K37L	K37Q	K37R	S41A	S41C
Mg·ATP	8.5	7.6	1.2	16	760	51	51	120	17	72

[a] The estimated errors are ±10%.

Table 6: Details of Crystallographic Data Collection and Refinement[a]

	S41A		S41C		K37Q	K37L
	AMPPCP + DAPA + Mn^{2+}	DAPA + Mn^{2+}	AMPPCP + DAPA + Mn^{2+}	DAPA + Mn^{2+}	AMPPCP + DAPA + Mn^{2+}	DAPA + Mn^{2+}
resolution (Å)	1.90	1.8	2.05	1.8	2.60	2.00
no. of reflections	16715	19497	13274	19343	6416	14162
completeness (%)	98.5	99.9	99.9	99.5	98.5	99.9
R-sym	0.060	0.060	0.082	0.068	0.077	0.083
R-factor (%)	23.8	23.8	17.8	22.8	15.3	19.0
R-free (%)	27.8	27.5	23.7	27.3	22.6	22.1
mean *B* (Å^2)	15.2	12.5	24.8	13.6	21.5	18.5
rmsd to wild type (Å)	0.16	0.19	0.24	0.22	0.19	0.21

[a] $R\text{-sym} = \sum_{hkl}\sum_i(I_i - \langle I\rangle)/\sum_{hkl}\sum_i(\langle I\rangle)$, where I_i is the scaled intensity of the ith observation, $\langle I\rangle$ is the mean intensity of this reflection, and rmsd represents root mean square differences in the Cα positions.

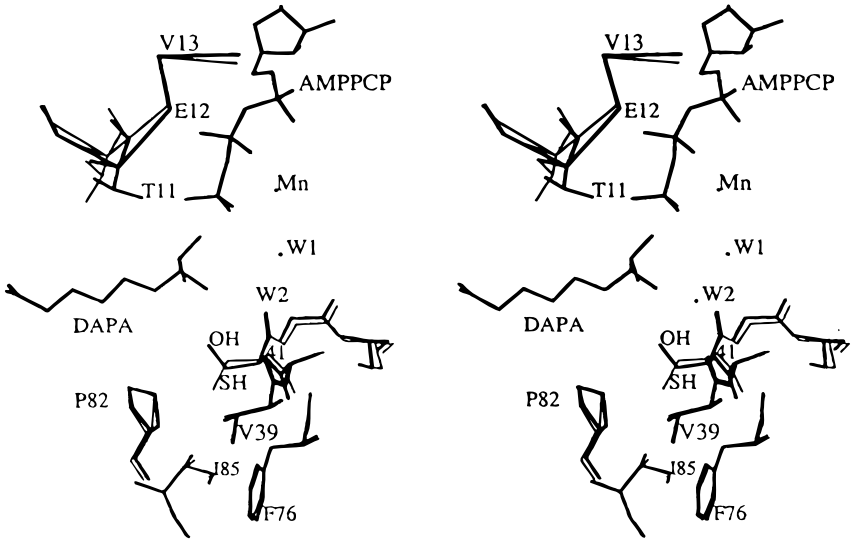

FIGURE 1: Stereoview illustrating the local conformational changes at postion 41 and the nearby region including the phosphate binding loop upon replacement of serine 41 with cysteine. Thick lines: wild-type enzyme. Thin lines: the S41C mutant enzyme.

density, especially in the diamino region. It has been shown that the carboxyl part of DAPA is anchored into place in a region where the two monomeric DTBS molecules come together to form one catalytically active dimer (Huang et al., 1995). Our data indicated that this is also true for the mutant enzymes. The interaction of the carboxyl group of DAPA with the other subunit was found to be the same in all four mutants and in the wild-type enzyme as indicated by the presence of clear electron density for this part of the substrate.

The side chain of Ser41 was proposed previously to form a hydrogen bond by accepting the H atom from the 7-amino group of DAPA. While absence of the hydroxyl group at residue 41 (S41A) resulted in no significant changes of the protein structure, but in poorer electron density for the diamino part of DAPA, replacement of the hydroxyl group with a thiol group (S41C) caused a local conformational change in the side chains of residue 41 and the nearby residues (Figure 1). The structure of S41C shows that the side chain of cysteine adopts a different conformation than Ser41: $\chi_1 = -64°$ and $+65°$ for cysteine and serine, respectively. The side chain of cysteine is directed out of the substrate binding site and buried in a hydrophobic environment among the side chains of Phe76, Ile85, and Val39. These changes may account for the higher K_m-(DAPA) and the reduced commitment of the DAPA−CO_2 complex. The polar serine adopts another conformation where the side chain is directed into the substrate binding site. This small difference in the conformation of the side chain of residue 41 results in slight differences in the position of surrounding residues. In particular, the side chain of Thr11 is a different rotamer in S41C than in the wild-type enzyme. This side chain is extremely important for the steady-state affinity of ATP (see Table 2). This might be the reason that S41C had a 4-fold higher K_m value for ATP (Table 2).

The structure of the mutants of Lys37 showed that these mutations did not significantly affect the position of the Cα atoms: the rmsd between both studied mutants and the wild-type enzyme is 0.18 Å. However, the poor electron density for DAPA in the Lys37 mutants (no density above 0.9σ for DAPA was observed anywhere except for the carboxyl group

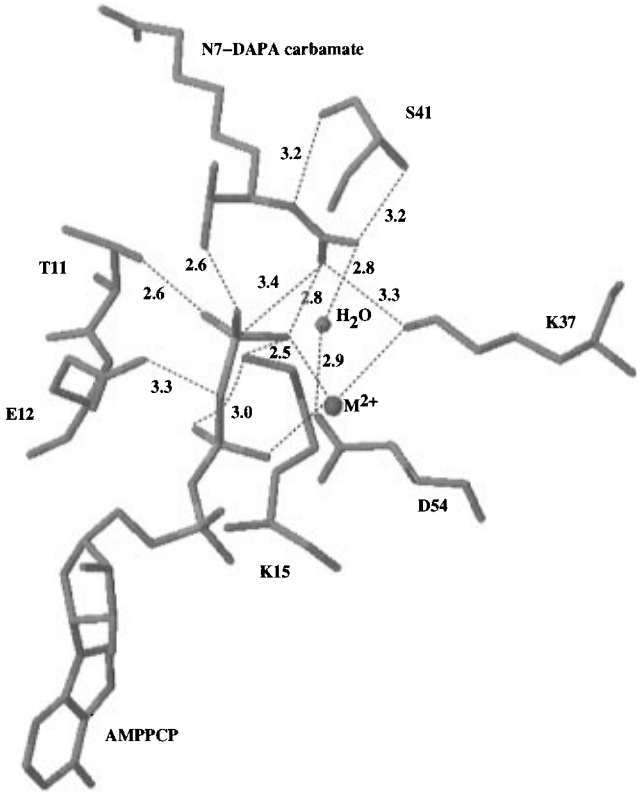

FIGURE 2: View of the interactions of AMPPCP and the N7-DAPA-carbamate with key enzymic residues and the metal ion at the active site of wild-type DTBS. Only enzymic groups with a potential role in catalysis are shown. Hydrogen bonds and salt bridges are indicated by dashed lines with the distances between heteroatoms (red, oxygen; blue, nitrogen; orange, phosphorus; green, carbon) in angstroms. Distances are based on the E·Ca·AMPPCP·DAPA complex (Huang et al., 1995). M^{2+} represents the active site metal ion.

of the molecule) means that the interaction of DAPA with these mutants cannot be described. It appears that DAPA adopts a rigid conformation in the active site only after carbamylation. The interaction of the negative charge of the N7-DAPA-carbamate with the positive charges of Lys37 in the substrate binding site helps to keep DAPA tightly bound in the active conformation.

The structure of both Lys37 mutants, on the other hand, showed that, in the absence of the positively charged side chain of residue 37, the position of the metal ion can shift up to 0.5 Å together with the side chains of Asp54 and Glu115. This result is not surprising since Lys37 is very close to all oxygen atoms coordinated to the metal ion: the distances between the NH_3 group of the side chain of Lys37 and O of the side chain carbonyl group of Glu115, O of the side chain carbonyl group of Asp54, and O of the side chain hydroxyl group of Thr16 in the wild-type enzyme are 2.94, 3.19, and 3.03 Å, respectively. Deletion of the positive side chain results in one more difference: the water molecule hydrogen bonded to one of the carbamate oxygens and to the side chain of Asp54 (see Figure 2), which was proposed to be very important for catalysis, is absent in the active site of both mutants.

DISCUSSION

The relative positions of the five enzymic residues, Thr11, Glu12, Lys15, Lys37, and Ser 41, with respect to the substrates in the *E. coli* DTBS active site are illustrated in Figure 2 and are based on the X-ray crystal structures of the complexes of DTBS with AMPPCP (a nonhydrolyzable ATP analogue) and the N7-DAPA-carbamate (Huang et al., 1995). These residues can be grouped into two general categories by their relative positions with respect to the different substrates: (1) residues in the DAPA-carbamate binding site (Lys37 and Ser41) and (2) residues in the ATP binding site (Thr11, Glu12, and Lys15). From the extensive crystallographic data (Huang et al., 1995), it was postulated that these five enzymic residues interact directly (or indirectly through a proton transfer system including active site bound water molecules) with substrates or intermediates through hydrogen bonds or salt bridges which facilitate the conversion of DAPA-carbamate to DTB (one possible mechanism is shown in Scheme 1).

Mutations in the DAPA-Carbamate Binding Site. The results of the mutagenesis and X-ray crystal structure experiments reported in this paper indicate that, of the two altered residues in the DAPA-carbamate binding site, only Lys37 may be considered catalytically essential. All three Lys37 mutant enzymes had reduced k_{cat}'s and elevated K_M's for both DAPA and ATP, with larger effects on the K_M (DAPA). The more dramatic changes in k_{cat} observed for K37R compared to K37L and K37Q could simply reflect a greater disruption of the active site scaffold caused by the more bulky arginine residue. Replacement of Lys37 by either glutamine or leucine also appeared to remove the overall forward commitment for the catalytic binary complex of E·DAPA-carbamate. However, as noted in the results, the failure to observe a burst of [^{14}C]DTB in the pulse−chase experiments may be a consequence of having insufficient ATP in the chase to trap a significant amount of the binary complex (Rose, 1980). We estimated that molar concentrations of ATP would be required to establish the appropriate conditions. Compared to the wild-type, the crystal structures of the K37L and K37Q mutants complexed with AMPPCP, DAPA, and either Mn^{2+} or Mg^{2+} showed similar binding of AMPPCP, less well defined binding of DAPA with no refinement of the diamino portion of the molecule, and a shift in the position of the metal ion. Loss of the positively charged side chain of Lys37 appeared to severely disrupt interactions between the enzyme active site and the carbonyl group of the carbamate moiety. Furthermore, the observed shift of the metal ion in the mutant enzyme active site could also result in a rearrangement of the charge distribution which would be expected to severely impair the formation of the Michaelis complex.

The S41A mutant had an elevated apparent K_M (DAPA) only at a subsaturating ATP concentration and showed no change in forward commitment for the E·DAPA-carbamate complex compared to wild-type, while the K_d(ATP) and K_M-(ATP) were both elevated. S41C, on the other hand, showed a more dramatic increase in the K_d(ATP) and the K_M's for DAPA at both saturating and subsaturating ATP levels and showed 3.7 times less forward commitment for the preformed E·DAPA-carbamate complex. The proposed hydrogen bond between the side chain of Ser41 and N7 of the DAPA-carbamate (as shown in Figure 2), thus, seems to be less important when all the substrates are tightly bound in the active site and is also a relatively weak interaction (at most a 10-fold effect on catalytic efficiency). The structure of S41C revealed a local conformational change caused by a flip of the side chain of Cys41 which could destabilize the

Michaelis complex *via* rotation of the side chains of Thr11 and other nearby residues (see Results, Figure 1). This perturbation of the active site region could account for the observed kinetic behavior of the S41C mutant. In contrast, S41A DTBS is kinetically and structurally very similar to the wild-type enzyme. The less dramatic effects on the kinetic parameters observed with the S41A mutant enzyme compared to S41C DTBS may be due to placement of a water molecule in the active site of S41A at the same position as the hydroxyl group of the wild-type. However, the current crystal structure of S41A could not identify this bound water molecule. We also expected to observe electron density for the DAPA-carbamate in the structure of S41A DTBS. The failure to detect the carbamate by X-ray crystallography suggests that the H-bond between S41 and the N7 of DAPA may be more important for stabilization of the DAPA carbamate in the crystal lattice than it is for binding and catalysis. Only one of many possible conformations for the carbamate binding site is revealed by the crystal structure, and that conformation may not be important for catalysis.

Mutations in the ATP Binding Site. All three altered residues in the ATP binding site are located on the highly conserved, mobile phosphate binding loop (Gly8-X-X-X-X-X-Gly14-Lys15-Thr16) (Huang et al., 1995). Lys15 is situated approximately equidistant between the β- and γ-phosphates of ATP (Figure 2) and, as such, would be expected to play a significant role in both catalysis, especially γ-phosphate transfer to the carbamate and stabilization of the phosphorylated intermediates, and binding of ATP. The K15Q mutant enzyme had a reduced k_{cat}, a higher K_d(ATP), and higher K_M's for both ATP and DAPA, with the more dramatic effect manifested on the K_M(ATP) consistent with the structural prediction.

Kinetic analyses of T11V showed that the catalytic efficiency for this mutant with respect to ATP was lowered by 5 orders of magnitude almost entirely by an increase in the K_M(ATP). Furthermore, T11V displayed altered pre-steady-state kinetics compared to the wild-type enzyme. T11V had a biphasic time course for the formation of both DTB and ADP, indicating an important role for this H-bond in catalysis by DTBS (G. Yang and A. Rendina, unpublished observations). Proximity of T11 to the γ-phosphate of ATP supports such a dramatic effect on binding of ATP in the Michaelis complex. One apparent reason for the elevated K_M and altered kinetics may be that the replacement of the hydroxyl side chain of Thr11 with a methyl group results in both the loss of a H-bond and an unfavorable van der Waals contact between the methyl group and the γ-phosphate of ATP. However, the unfavorable van der Waals contact in T11V seemed unlikely since the K_d(ATP) is unchanged (Table 5). Both the K_d and K_M(ATP) for T11V would be expected to be elevated by this unfavorable contact because the configuration of the nucleotide binding site is the same in both the binary complex of DTBS·ADP and the ternary complex of DTBS·ACP·DAPA in wild-type DTBS (Huang et al., 1995). The recently solved structures of native T11V and the ternary complex of T11V·ACP·DAPA show that there are no changes in the position of the nucleotide compared to the wild-type enzyme and suggest that the methyl group of Val11 does not interfere with the binding of ATP (T. Sandalova and Y. Lindqvist, unpublished observations). Having argued against an unfavorable van der Waals contact, the observed properties of T11V must be explained by the loss of a single H-bond. In the crystal structure for the wild-type DTBS·DAPA·CaAMPPCP complex the distance between the side chain of Thr11 and one of the oxygens of the γ-phosphate of ATP is very short, about 2.56 Å, further suggesting that the hydrogen bond may be unusually strong. One possibility is that this H-bond may be a low-barrier hydrogen bond (LBHB) (Cleland, 1992; Gerlt, 1994; Gerlt & Gassman, 1993; Frey et al., 1994; Cleland & Kreevoy, 1994, 1995; Frey, 1995) which could account for the 10^5 reduction in k_{cat}/K_M for ATP and the altered transient kinetics of the T11V enzyme. However, a preliminary NMR study with wild-type DTBS in the presence of saturating levels of DAPA, CO_2, AMPPCP and Mg^{2+} failed to reveal any ^{1}H NMR signals in the downfield region of the spectrum ($\delta_H = 10-20$ ppm), which has been one of the most unambiguous methods for characterizing LBHB's (Hibbert & Emsley, 1990). Although it is not clear at present what causes the dramatic changes in the kinetic properties of the T11V mutant, the H-bond between the hydroxyl group of Thr11 and the oxygen of the γ-phosphate of ATP is obviously crucial for the enzyme's catalytic efficiency.

An earlier study (Huang et al., 1995) showed that, upon binding of nucleotide, the phosphate binding loop moves closer to the substrates, such that the side chain of Glu12, instead of forming a salt bridge to Lys148 as in the free wild-type DTBS, undergoes a significant conformational change and points into the active sites toward the β-phosphate of ATP and N8 of the DAPA-carbamate. Our results with mutants of Glu12 ruled out involvement of this residue either in protonation of the bridging oxygen of ATP to facilitate phosphate transfer or in deprotonation of the N8 nitrogen of the phosphorylated tetrahedral intermediate after cyclization [potential roles suggested in Huang et al. (1995)]. However, the E12A enzyme had the same apparent K_M values for DAPA at saturating and subsaturating ATP concentrations, indicating a possible role for Glu12 in the synergy between ATP and DAPA observed in the wild-type DTBS. A possible explanation is that movement of the loop region is both enthalpically (breakage of the salt bridge between Glu12 and Lys148) and entropically unfavorable to the formation of the correct active site geometry in wild-type DTBS. Tight binding of substrates to DTBS appears to rely on the correct position of this loop domain. In E12A, no salt bridge between Lys148 and Ala12 can be formed. Therefore, the conformation of the loop domain in empty E12A may be quite similar to that in E12A complexed with the substrates. The observation of 6-fold *tighter* binding of ATP to E12A (K_d, Table 5) clearly supports this argument. In addition, the 100% trapping of the committed E·DAPA·CO_2 complex for E12A (86% for wild-type, Table 4) indicates that the movement of this loop domain could also be important for the overall turnover of DTBS. This implies that a conformational change step may occur in the reaction scheme of DTBS and provides the basis for further studies of the effects of the mutations on the kinetic reaction pathway of DTBS.

Although more detailed work is needed, the mutant enzymes studied here have not identified a likely candidate for a catalytic base. After the N7-carbamate is formed and/or bound to the enzyme, the N8 nitrogen must be deprotonated both prior and subsequent to cyclization (Scheme 1). The enzyme does not appear to participate directly in these deprotonations; rather, it seems that the role of the enzyme is to properly position the substrates and neutralize the

negative charges in both substrates and intermediates *via* the divalent metal cation and the two key lysine residues. The deprotonations of the N8 nitrogen could be achieved by interactions with the γ-phosphate of ATP prior to cyclization and, again, by intramolecular proton transfer from the protonated cyclic intermediate to the leaving phosphate group. Note that formation of the phosphorylated carbamate would also be facilitated by donation of a proton from N8 to the γ-phosphate of ATP. A similar substrate-assisted reaction mechanism has been suggested and established recently by Warshel and co-workers for the $p21^{ras}$-mediated hydrolysis of GTP in which the substrate of the reaction, GTP, acts as a base catalyst (Schweins & Warshel, 1996; Schweins et al., 1994, 1995, 1996). This mechanistic strategy appears to have been adopted by other enzyme systems as well, such as transducin α (Sondek et al., 1994) and myosin (Fisher et al., 1995).

ACKNOWLEDGMENT

We thank Katharine Gibson, George Lorimer, Wendy Taylor, Doug Jordan, James Thompson, Lynn Abell, and Gunter Schneider for reviewing the manuscript and for many helpful comments. The assistance of Hongji Chi for help with enzyme purification, Jim Doughty and Bob Livingston for electrospray mass spectroscopy, and Bruce Lockett for the ^{1}H NMR study is greatly appreciated. We also thank Steve Vollmer for sequence alignments, James Chen for structural models of the yeast and *Synechocystis* DTBS enzymes based on their primary amino acid sequences, and Kevin Kranis for helping us visualize the structures.

SUPPORTING INFORMATION AVAILABLE

Details of the construction of the BL21(bioD::NPTII, DE3) host strain used in the overexpression of the recombinant DTBS enzymes and a table (Table 1) listing the mutants generated, inside and outside primers, amino acid substitutions, and restriction enzymes (3 pages). Ordering information is given on any current masthead page.

REFERENCES

Alexeev, D., Baxter, R. L., Smekal, O., & Sawyer, L. (1995) *Structure 3*, 1207.
Balbas, P., Alexeyev, M., Shokolenko, I., Alvarado, X., Gosset, G., Bolivar, F., & Valle, R. (1993) *Gene 136*, 211.
Baldet, P., Gerbling, H., Axiotis, S., & Douce, R. (1993) *Eur. J. Biochem. 217*, 479.
Brunger, A. T. (1990) *Acta Crystallogr. A46*, 46.
Cleland, W. W. (1979a) *Anal. Biochem. 99*, 142.
Cleland, W. W. (1979b) *Methods Enzymol. 63*, 103.
Cleland, W. W. (1992) *Biochemistry 31*, 317.
Cleland, W. W., & Kreevoy, M. (1994) *Science 264*, 1887.
Cleland, W. W., & Kreevoy, M. (1995) *Science 269*, 104.
Eisenberg, M. A. (1973) *Adv. Enzymol. 38*, 317.
Erlich, H. A., Ed., (1992) *PCR Technology Principles and Applications for DNA Amplification*, W. H. Freeman and Co., New York.
Fisher, A. H., Smith, C. A., Thoden, J. B., Smith, R., Sutoh, K., Holden, H. M., & Rayment, I. (1995) *Biochemistry 34*, 8960.
Frey, P. A. (1995) *Science 269*, 104.
Frey, P. A., Whitt, S. A., & Tobin, J. B. (1994) *Science 264*, 1927.
Gerlt, J. A. (1994) *Curr. Opin. Struct. Biol. 4*, 593.
Gerlt, J. A., & Gassman, P. G. (1993) *Biochemistry 32*, 11943.
Gibson, K. J., Lorimer, G. H., Rendina, A. R., Taylor, W. S., Cohen, G., Gatenby, A. A., Payne, W. G., Christopher Roe, D., Lockett, B. A., Nudelman, A., Marcovici, D., Nachum, A., Wexler, B. A., Marsilii, E. L., Turner, Sr., I. M., Howe, L. D., Kalbach, C. E., & Chi, H. (1995) *Biochemistry 34*, 10976.
Hibbert, F., & Emsley, J. (1990) *Adv. Phys. Org. Chem. 26*, 255.
Huang, W., Lindqvist, Y., Schneider, G., Gibson, K., Flint, D., & Lorimer, G. (1994) *Structure 2*, 407.
Huang, W., Jia, J., Gibson, K. J., Taylor, W. S., Rendina, A. R., Schneider, G., & Lindqvist, Y. (1995) *Biochemistry 34*, 10985.
Jones, T. A., Zou, J. Y., Cowan, S. W., & Kjeldgaard, M. (1991) *Acta Crystallogr. A47*, 110.
Krell, M., & Eisenberg, M. A. (1970) *J. Biol. Chem. 245*, 6558.
Miller, J. H. (1992) in *A Short Course in Bacterial Genetics*, Cold Spring Harbor Laboratory Press, New York.
Ormö, M., & Sjöberg, B.-M. (1990) *Anal. Biochem. 189*, 138.
Otwinowski, Z. (1993) in *Data Collection and Processing, Proceedings of the CCP4 Study Weekend*, pp 56−62, Daresbury Laboratory, Warrington, U.K.
Rose, I. A. (1980) *Methods Enzymol. 64*, 47−59.
Sambrook, J., Fritsch, E. F., & Maniatis, T. (1989) in *Molecular Cloning*, Cold Spring Harbor Laboratory Press, Plainview, NY.
Sanger, F., Milken, S., & Coulson, A. R. (1977) *Proc. Natl. Acad. Sci. U.S.A. 74*, 5463.
Schweins, T., & Warshel, A. (1996) *Biochemistry 35*, 14232.
Schweins, T., Langen, R., & Warshel, A. (1994) *Nat. Struct. Biol. 1*, 476.
Schweins, T., T., Geyer, M., Scheffzek, K., Warshel, A., Kalbitzer, H. R., & Wittinghofer, A. (1995) *Nat. Struct. Biol. 2*, 36.
Schweins, T., Geyer, M., Kalbitzer, H. R., Wittinghofer, A., & Warshel, A. (1996) *Biochemistry 35*, 14225.
Sondek, J., Lambright, D. G., Noel, J. P., Hamm, H. E., & Sigler, P. B. (1994) *Nature 372*, 276.

BI9631677